CrossMark

ARTICLE

In vitro bioactivity and antibacterial properties of bismuth oxide modified bioactive glasses

Sakthi Prasad S
Academy of Scientific and Innovative Research (AcSIR), Campus: CSIR-Central Glass & Ceramic Research Institute, Kolkata-700 032, India; and Glass Division, CSIR-Central Glass & Ceramic Research Institute, Kolkata-700 032, India

Itishree Ratha
Bioceramics and Coating Division, CSIR-Central Glass & Ceramic Research Institute, Kolkata-700 032, India

Tarun Adarsh
Ram Lal Anand College, Delhi University, New Delhi-110 021, India

Akrity Anand
Bioceramics and Coating Division, CSIR-Central Glass & Ceramic Research Institute, Kolkata-700 032, India

Prasanta Kumar Sinha
Academy of Scientific and Innovative Research (AcSIR), Campus: CSIR-Central Glass & Ceramic Research Institute, Kolkata-700 032, India; and Materials Characterization & Instrumentation Division, CSIR-Central Glass & Ceramic Research Institute, Kolkata-700 032, India

Prerna Diwan
Ram Lal Anand College, Delhi University, New Delhi-110 021, India

Kalyandurg Annapurna and Kaushik Biswas[a)]
Academy of Scientific and Innovative Research (AcSIR), Campus: CSIR-Central Glass & Ceramic Research Institute, Kolkata-700 032, India; and Glass Division, CSIR-Central Glass & Ceramic Research Institute, Kolkata-700 032, India

(Received 6 September 2017; accepted 8 November 2017)

Chronic osteomyelitis, a bone infection caused by bacteria, requires extensive parenteral treatments. With an aim to develop bioactive glass with antibacterial properties to resist such infections, bioactive glasses with bismuth oxide as the dopant in various amounts up to 8 wt% were prepared. X-ray diffraction patterns and Fourier-transform infrared spectra of glass samples after immersion in simulated body fluid showed the presence of hydroxyapatite (HAp) and hydroxyl carbonate apatite for all samples except with the one having Bi_2O_3 substitution of 8 wt%. In vitro cell proliferation by MTT assay studies using a mouse fibroblast cell line (NIH3T3) have also been carried out. Primary antimicrobial activity of the glass particles was analyzed against *Escherichia coli* (*E. coli*) using broth microdilution method which exhibited bacteriostatic effects and bactericidal properties in selected samples. The combination of bioactivity, cell proliferation, and antibacterial properties of selected Bismuth-containing bioactive glasses could be exploited in treating bone-related infections.

I. INTRODUCTION

Bioactive glasses have a wide range of clinical applications in the field of orthopedics for the repair and regeneration of bone, dentistry for teeth repair, and treatment against diseases like osteoporosis and osteomyelitis.[1] Bioactive glasses bond to bone due to their ability to form an interface that helps in biological fixation with the natural bone.[2] The interface is formed when the surface of the bioactive glass interacts with the physiological environment inside the body and is found to be made of biologically active hydroxyl carbonate apatite (HCA), which is chemically and structurally similar to the apatite mineral of natural bone.[2] Hench developed first bioactive glass in SiO_2–Na_2O–CaO–P_2O_5 system known as 45S5 (Bioglass®) which has been commercially used for many bone-related treatments. Other glasses like S53P4 (BonAlive®)[3] and 13-93[4] were commercially developed for synthetic bone graft applications.

Bioactive glasses when added with ions exhibiting antibacterial properties can be advantageous in treatments of bacterial infected bones. Osteomyelitis is a bone disease caused by infectious microorganisms and occurs in the form of inflammation around the bone resulting in

Contributing Editor: Amit Bandyopadhyay
[a)]Address all correspondence to this author.
e-mail: kbiswas@cgcri.res.in
DOI: 10.1557/jmr.2017.442

 © Materials Research Society 2017

https://doi.org/10.1557/jmr.2017.442 Published online by Cambridge University Press

bone destruction.[5] Usually, treatment of osteomyelitis involves removal of the infected part and treating it with antibiotics like penicillin, methicillin, oxacillin, and amoxicillin. But, recently these bacteria have shown resistance to these antibiotics and emerged as methicillin-resistant *Staphylococcus aureus* (MRSA) making the treatment of osteomyelitis difficult.[5,6] A material that can heal the bone defect as well as prevent the bacterial infections in the infected zone could be a better choice for the osteomyelitis treatment. In this regard, a bioactive glass showing bone bonding, bone regeneration, and antibacterial properties could be a better material for treating osteomyelitis.[7]

The bioactive glasses (e.g., S53P4) without the addition of any antibacterial ions can show antibacterial properties either due to the effect of increase in pH in the surrounding medium resulting from the release of Na^+ and Ca^{2+} ions.[8] To get a long-term and effective antibacterial effect, the glasses have to be doped with ions exhibiting broad spectrum antibacterial action.[9] Many research groups have studied the effect of antibacterial ions like silver (Ag^+), cerium (Ce^{3+}), and copper (Cu^+) ions doped in the bioactive glass systems against various bacteria like *Escherichia coli*, *Staphylococcus aureus*, *Pseudomonas aeruginosa*, and *Streptococcus sanguis*.[9–15]

Though, the antibacterial effects of various ions in bioactive glasses have been studied by many research groups, the effect of bismuth ions for improving antibacterial properties in bioactive glasses has not yet been explored even after the wide usage of bismuth compounds in gasteroenterology[16] in treating stomach-related diseases and its antimicrobial properties in the treatment against bacterial infections caused by *H. pylori* in the gut.[17]

Lambert and Midolo have discussed various mechanisms by which bismuth ions exhibit bactericidal effects against the *H. pylori* bacteria.[17] Bismuth-added calcium silicate-based mineral trioxide aggregate (MTA) had been widely used as the dental filling. This MTA has shown biocompatibility, radiopacity, cell proliferation, and antibacterial properties.[18,19] Bismuth ions replacing calcium ions in substituted hydroxyapatite has shown better osteoblast proliferation and increased alkaline phosphatise activity.[20] Inhibition toward both Gram positive *S. aureus* and Gram negative *E. coli* was observed in bismuth-substituted HAp.[21] Bi_2O_3 was successfully added to nano-bioactive glass powders of 45S5 glass composition using flame spray process by 20 and 50 wt%, and these were found to be radiopaque to X-rays along with improved apatite formation.[22,23]

The present work aims to elucidate the effect of progressive bismuth oxide incorporation substituting SiO_2 and Na_2O in S53P4 glass composition on the structural, thermal, and physical properties. The prepared glasses were also studied for their surface apatite formation in in vitro bioactivity studies, cell proliferation, and antibacterial properties.

II. MATERIALS AND METHODS

A. Glass synthesis using melt-quench technique

The glasses were prepared in the system SiO_2–Na_2O–CaO–P_2O_5–Bi_2O_3 using melt-quench technique. The compositions of glasses in both wt% and mol% for the present study is given in Table I which has base glass (B0) and four glasses B1, B2, B4, and B8 having bismuth oxide equally substituting SiO_2 and Na_2O together in 1 wt%, 2 wt%, 4 wt%, and 8 wt%, respectively.

The glasses were prepared from a batch of fine chemicals such as SiO_2 (99.8%, Sipur A1 Bremtheler Quartz-itwerk, Usingen, Germany), Na_2CO_3 (99.5%, Merck, Mumbai, India), $CaCO_3$ (99%, Sigma Aldrich, Tokyo, Japan), $CaHPO_4{\cdot}2H_2O$ (98%, Sigma Aldrich, Steinheim, Germany) and Bi_2O_3 (99.9%, Sigma Aldrich, Steinheim, Germany). The batches were prepared for 100 g glass from each composition, and weighed chemicals were mixed thoroughly. These batches were charged in a platinum crucible at 1300 °C, and melting was done at 1450 °C in a raising hearth furnace. The molten batches were homogenized by stirring manually twice using a fused silica rod with a 45 min time interval. The molten batches were then casted on a stainless steel mold of length 88 mm and width 30 mm to get glass blocks. These glass blocks were annealed in the annealing furnace at 520 °C for 2 h and cooled slowly to room temperature. The as-prepared glass samples were cut into cuboid pieces having 10 mm length, 10 mm width, and a thickness of 2 mm and also circular discs of 10 mm diameter and thickness of 2 mm followed by rough and fine polishing. Glass powders were prepared by grinding crushed glass pieces using mortar and pestle and sieved through a 45 μm mesh. These powdered glass samples were characterised for X-ray diffraction (XRD), Fourier-transform infrared (FTIR) spectroscopy, mechanical, physical, and thermal properties followed by in vitro bioactivity, ion release studies, cell proliferation, and antibacterial studies. After immersing the samples in a simulated body fluid (SBF) solution, the surfaces of the glasses were investigated for phase and microstructural analysis, while the SBF supernatant was used for ion release studies.

B. X-ray diffraction (XRD)

The amorphous nature of the as-prepared glass powders and crystalline phase identification in glass powders subjected to immersion in SBF solution were examined on X-Ray Diffractometer (Ultima IV, Rigaku, Tokyo, Japan) with X'Celerator operating at 40 kV and 30 mA using Ni-filtered Cu K_α radiation having a wave length of 1.5418 Å.

C. Fourier-transform infrared (FTIR) spectroscopy

FTIR transmission spectra of as-prepared glass powders as well as glass powders subjected to immersion in the SBF solution were recorded in mid-infrared (MIR)

https://doi.org/10.1557/jmr.2017.442 Published online by Cambridge University Press

TABLE I. Composition of base glass and bismuth oxide substituted glasses in wt% and mol%.

	B0		B1		B2		B4		B8	
	wt%	mol%	wt%	mol%	wt%	mol%	wt%	mol%	wt%	mol%
SiO_2	53	53.85	52.5	53.81	52	53.77	51	53.69	49	53.51
Na_2O	23	22.65	22.5	22.36	22	22.05	21	21.43	19	20.11
CaO	20	21.77	20	21.96	20	22.16	20	22.56	20	23.4
P_2O_5	4	1.72	4	1.74	4	1.75	4	1.78	4	1.85
Bi_2O_3	0	0	1	0.13	2	0.27	4	0.54	8	1.13

(4000–400 cm^{-1}) using the FTIR/FIR spectrophotometer (Frontier IRL 1280119; Perkin Elmer, Waltham, MA). The sample powders were mixed with KBr (ratio 1:100) and pelletised followed by analysis in transmission mode.

D. Differential scanning calorimetry

The differential scanning calorimetry (DSC) analysis of glass powders was performed using a simultaneous thermal analyzer (model: STA 449F3, Netzsch GmbH, Selb, Germany) at a heating rate of 10 K/min. 20–30 mg of glass powders were taken in Pt–Ir crucibles for DSC analysis.

E. Density measurement

The density (ρ) values of glass samples were measured on a Mettler-Tolledo analytical balance (Model: AB-204-S/FACT, Mettler Toledo, Greifensee, Switzerland) fitted with a density measurement kit by applying the Archimedes' buoyancy principle using double distilled water as an immersion liquid.

F. In vitro bioactivity studies

In vitro bioactivity studies were carried out using the SBF solution having pH 7.4 at a temperature of 37.4 °C. The SBF was prepared using the standard method described by Kokubo et al. using the standard reagents.[24] The powder samples were studied in the SBF solution in the ratio of 150 mg per 100 mL in polymer bottles and kept inside an incubator maintaining a uniform temperature of 37.4 °C. These samples were analyzed for 1, 3, 7, and 14 days immersion for apatite formation through XRD and FTIR characterization techniques. To understand the microstructure of the surface layer, field emission scanning electron microscope (FESEM) measurements were carried out on bulk samples using instrument Carl Zeiss FESEM Supra 35 VP (ZEISS, Oberkochen, Germany). The bulk glass samples were prepared by covering all surfaces except the top surface with wax such that the surface area of 100 mm^2 will be exposed to the SBF solution. These samples were placed in polymer tubes containing 15 mL of SBF solution with the uncoated surface facing up which was kept inside the incubator maintaining a uniform temperature of 37.4 °C and studied for 7 and 14 days. It is important to mention that to understand the comparative apatite forming tendency of different glasses, the immersion time in SBF was extended up to 14 days, while the actual pH (7.4) of the SBF solution is expected to alter with the increase in immersion time. The blank SBF solution was estimated for the pH values and Si^{4+}, Na^+, P^{5+}, and Bi^{3+} ion concentrations. The pH value measurements were done using a pH meter (L1-1122pH, LABARD, Kolkata, India) at 37.4 °C in triplicates, and the average values are reported. For each ion, samples were done in duplicates, and the average values were reported. The Si^{4+} and P^{5+} ion concentration in the blank SBF solution and SBF supernatant were estimated by colorimetric methods using UV-Vis double beam spectrophotometer (AU 2701, Syntronics, Ahmedabad, India). The concentration of Na^+ ions in the blank SBF solution and SBF supernatant was estimated using a flame emission photometer (Mediflame 127, Syntronics, Ahmedabad, India). The Bi^{3+} ion concentration in the SBF supernatant was measured using the inductively coupled plasma—mass spectroscopy (ICP-MS) instrument (NexIon 300X ICP-MS, Perkin-Elmer, Waltham, Massachusetts). In determining the Bi^{3+} ion concentration in the ICP-MS instrument, calibration was done using the standard Bi^{3+} ion containing solution.

G. In vitro cell proliferation studies

In vitro cell proliferation test of the bulk glass samples was evaluated for 3, 7, and 11 day culture periods using the mouse embryonic fibroblast cell line (NIH3T3). The dimension of the samples used for this test was 10 × 10 × 2 mm^3. All the samples were sterilized in an autoclave at 15 psi pressure and at 121 °C before cell culture study. For comparison, experiments were carried out on triplicate samples and placed in a 24-well plate, seeded with 5×10^3 cells/well. After 4 h of cell seeding, 1 mL of aliquot growth media containing Dulbecco's modified Eagle's medium cell media supplemented with 10% fetal bovine serum and 0.1% penicillin and streptomycin (1:1 ratio) antibiotic solutions was added to each well and placed in an incubator at 37 °C under an atmosphere of 95% humidified air and 5% CO_2. The culture medium was changed for every three days throughout the duration of the experiment. The in vitro

https://doi.org/10.1557/jmr.2017.442 Published online by Cambridge University Press

cytotoxicity of bioactive glass samples was assessed using an MTT assay following the standard protocol.[25,26] The optical density (OD) absorbance was measured by an ELISA plate reader (Bio rad, iMark™, Tokyo, Japan) at 595 nm. The mean, standard deviation (SD), and standard error (SE) values for the obtained OD values were calculated, and the mean ± SE plotted with time (days) for each glass sample and base glass (B0) was considered as the control. For each sample, the statistical significance was set at $P < 0.05$ and validated using the P value from the Student's t-test with respect to the base glass (B0) considering the one-tailed hypothesis with two independent samples having equal variance and 95% confidence level.

H. Antibacterial studies using broth microdilution method

The broth microdilution method was modified from the standard method provided by the European committee for antimicrobial susceptibility testing (EUCAST) to test the glass samples.[27] The glass powder samples were used to study the antibacterial effects against the Gram-negative bacterium *E. coli* (ATCC 25922) strain. The stock suspension was prepared by mixing 1 mL *E. coli* with 9 mL of autoclaved Mueller-Hinton Broth (MHB) and incubated at 37 °C with continuous shaking at 200 rpm till it reached the OD at 595 nm (OD) of 0.3. The stock suspension was again diluted with sterile MHB to obtain the OD value of 0.03, and the glass powder samples were autoclaved. 0.02 g from each autoclaved powder sample was poured (in triplicates) in the 96-well micro titer plate. Base glass powder was assigned as positive control, while the *E. coli* suspension without any glass powder sample was assigned as negative control in the template. 200 μL of the *E. coli* suspension was pipetted and mixed with the glass powder samples in each well to achieve 100 mg/mL concentration, and the 0 h-OD reading was taken. The plate was placed in an incubator at 37 °C and subsequent OD readings after 1 and 2 h were recorded. After 24 h of incubation, 100 μL of the mixture was pipetted and spread out on Mueller-Hinton agar (MHA) Petri-plates in triplicates to verify the bactericidal property of the glass powder samples. The MHA plates were then incubated overnight at 37 °C, and the colony forming units (CFUs) in each agar plate were counted next day. The bactericidal activity of the glass samples was studied from the reduction in the CFU on the agar plates compared to the initial CFU in the bacterial suspension. To check the inhibition of bacterial growth (bacteriostatic property of the glass powder samples) of the samples, ΔOD values for each of the glass powder mixed bacterial suspension were calculated by subtracting the 0 h-OD readings from the obtained OD reading. The mean, standard deviation (SD), and standard error (SE) values for the ΔOD values were calculated and the mean ± SE are plotted with their time of incubation (h) for each glass powder samples along with the positive and negative controls for comparison. Each sample was tested with respect to the negative control for statistical significance ($P < 0.05$) determined from the Student's t-test (one-tailed hypothesis, two independent samples having equal variance and 95% confidence level).

III. RESULTS

A. X-ray diffraction (XRD) analysis

The XRD patterns obtained for all the powder samples of the melt-quenched glasses as shown in Fig. 1(a) exhibit typical broad halos indicating the complete amorphous nature. The XRD patterns of the glasses after immersion in the SBF solution for 1 day exhibited broad halos showing no indication of any crystalline phases (not shown in Fig. 1). After immersion in the SBF solution for 3, 7, and 14 days, the XRD patterns of certain glasses have shown sharp diffraction peaks as presented in Figs. 1(b)–1(d), respectively, depending on the glass composition. The peaks have been identified and assigned to standard hexagonal HAp (JCPDS: 09-0432) and HCA (JCPDS: 04-0697) crystalline phases. The presence of a broad halo occurring at around $2\theta = 22.5°$ along with the sharp crystalline peaks of all the samples matches with the XRD pattern of the Si–O–Si gel layer[28] confirming the formation of the silica gel layer along with HAp and HCA. From Figs. 1(b) and 1(c), it can be observed that XRD patterns of B0, B1, and B2 samples have shown well-defined peaks of HAp and HCA phases after immersing in the SBF solution for 3 and 7 days, while XRD patterns of the B4 and B8 samples are dominated by broad halos indicating the lack of formation of HAp and HCA. In Fig. 1(d), after 14 days immersion, well-defined peaks of HAp and HCA phases are observed for all the glass samples except in the B8 sample indicating the lack of apatite formation.

B. Fourier-transform infrared (FTIR) spectroscopy studies

The FTIR transmission spectra of the melt-quenched glass samples in Fig. 2(a) show various vibrational bands corresponding to Si–O–Si bond vibrations. The bands at 1060 and 922 cm^{-1} are assigned to Si–O–Si asymmetric stretching and Si-NBO stretching, respectively. The band at around 755 cm^{-1} corresponds to Si–O–Si symmetric stretching vibrations. The bands occurring at 590 and 464 cm^{-1} correspond to the bending modes of O–Si–O and Si–O–Si bonds, respectively.[29]

The FTIR transmission spectra of different glass powders after immersion studies in SBF solution for 3, 7, and 14 days are shown in Figs. 2(b)–2(d), respectively. The vibrational bands corresponding to Si–O–Si bonds,

https://doi.org/10.1557/jmr.2017.442 Published online by Cambridge University Press

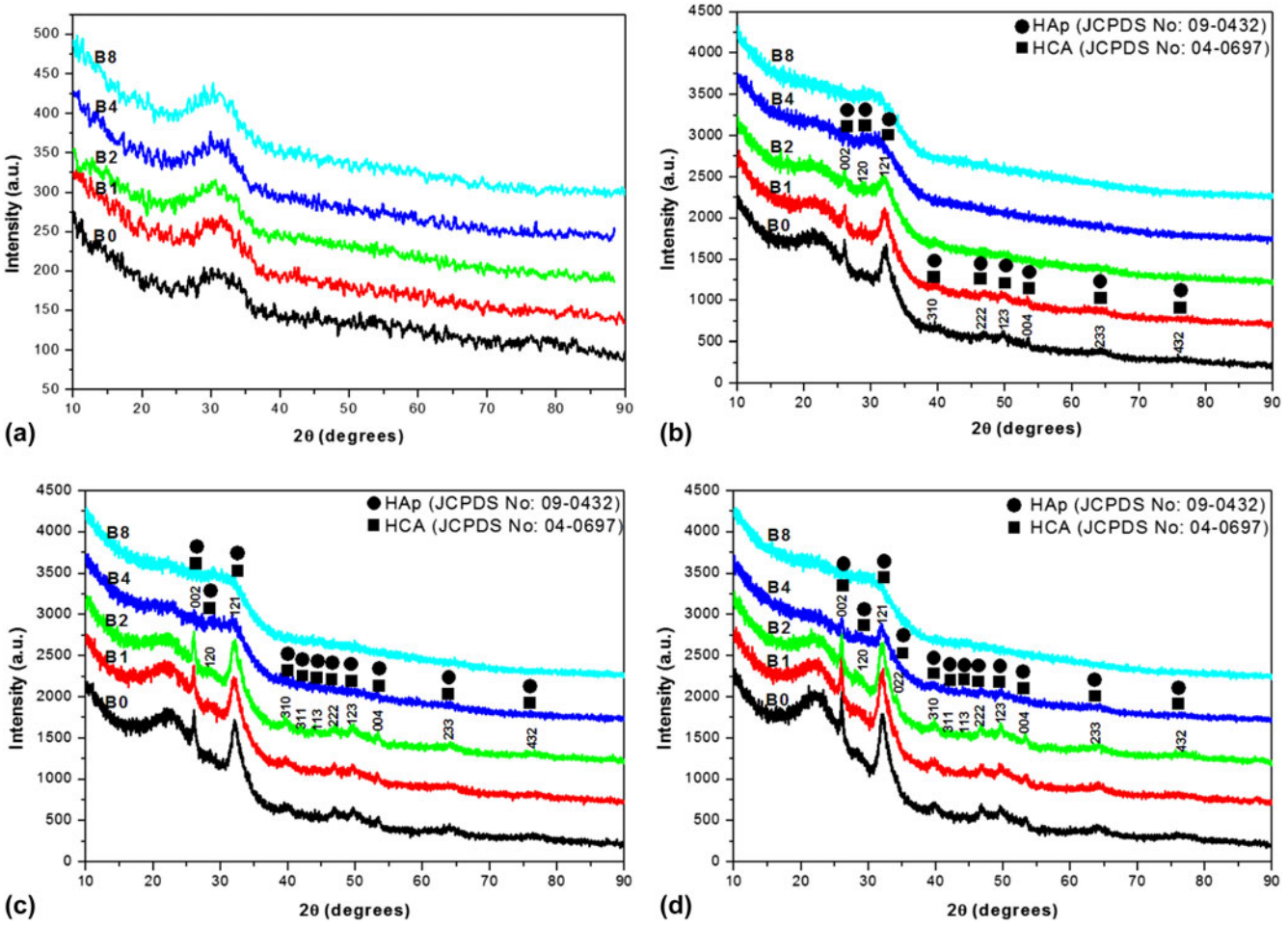


FIG. 1. The XRD pattern of (a) melt-quenched glass powders; the XRD pattern of glass powders after immersion in the SBF solution for (b) 3 days, (c) 7 days, and (d) 14 days.

$(PO_4)^{3-}$, $(CO_3)^{2,-}$ and molecular water were identified in the FTIR spectra[29–31] of certain samples depending on the composition. The band occurring at 3448 cm^{-1} corresponds to molecular water vibrations. The bands occurring at 1645 and 1750 cm^{-1} are due to the presence of molecular water. The bands occurring at 1413 and 1470 cm^{-1} are due to asymmetric stretching vibrations of the $(CO_3)^{2-}$ unit while 873 cm^{-1} represents bending vibrations of the $(CO_3)^{2-}$ unit. This confirms that the apatite is of B-type HCA in which $(CO_3)^{2-}$ units partially substitute $(PO_4)^{3-}$ units in the HAp lattice. The bands at 1095 and 1035 cm^{-1} are assigned to asymmetric stretching of the P–O bond in the $(PO_4)^{3-}$ units, while the band at 960 cm^{-1} is assigned to the symmetric stretching mode of the P–O bond in the $(PO_4)^{3-}$ units. The bands at 606 and 566 cm^{-1} are assigned to P–O bond bending in the $(PO_4)^{3-}$ units.

The bands occurring at 1249, 1064, 800, and 468 cm^{-1} correspond to out-of-plane asymmetric stretching, in-plane asymmetric stretching, symmetric stretching, and bending of Si–O–Si, respectively. From Fig. 2(b), it is observed that all the samples after 3 days of immersion show similar bands corresponding to Si–O stretching and bending as well as molecular water vibrations. But the presence of P–O bending and C–O bond stretching is more dominant in the base glass (B0) sample and decreases with the gradual incorporation of Bi_2O_3. However, the asymmetric stretching mode of the P–O bond cannot be well defined as it is overlapped with the vibrational bands of Si–O–Si asymmetric stretching. In Fig. 2(c), it is observed that after immersion in the SBF solution for 7 days, the intensity of all the bands related to the P–O bond is found to be increased compared to that of the samples after immersion in the SBF solution for 3 days. Also, the P–O asymmetric stretching band in samples immersed in the SBF solution for 7 days has become distinct. Furthermore, the bands corresponding to P–O bending and stretching, Si–O–Si symmetric stretching, and C–O bond bending stretching are more dominant in the base glass (B0) and gradually reduces with the incorporation of bismuth oxide. From Fig. 2(d), the glass powders after immersion in the SBF solution for 14 days,

https://doi.org/10.1557/jmr.2017.442 Published online by Cambridge University Press

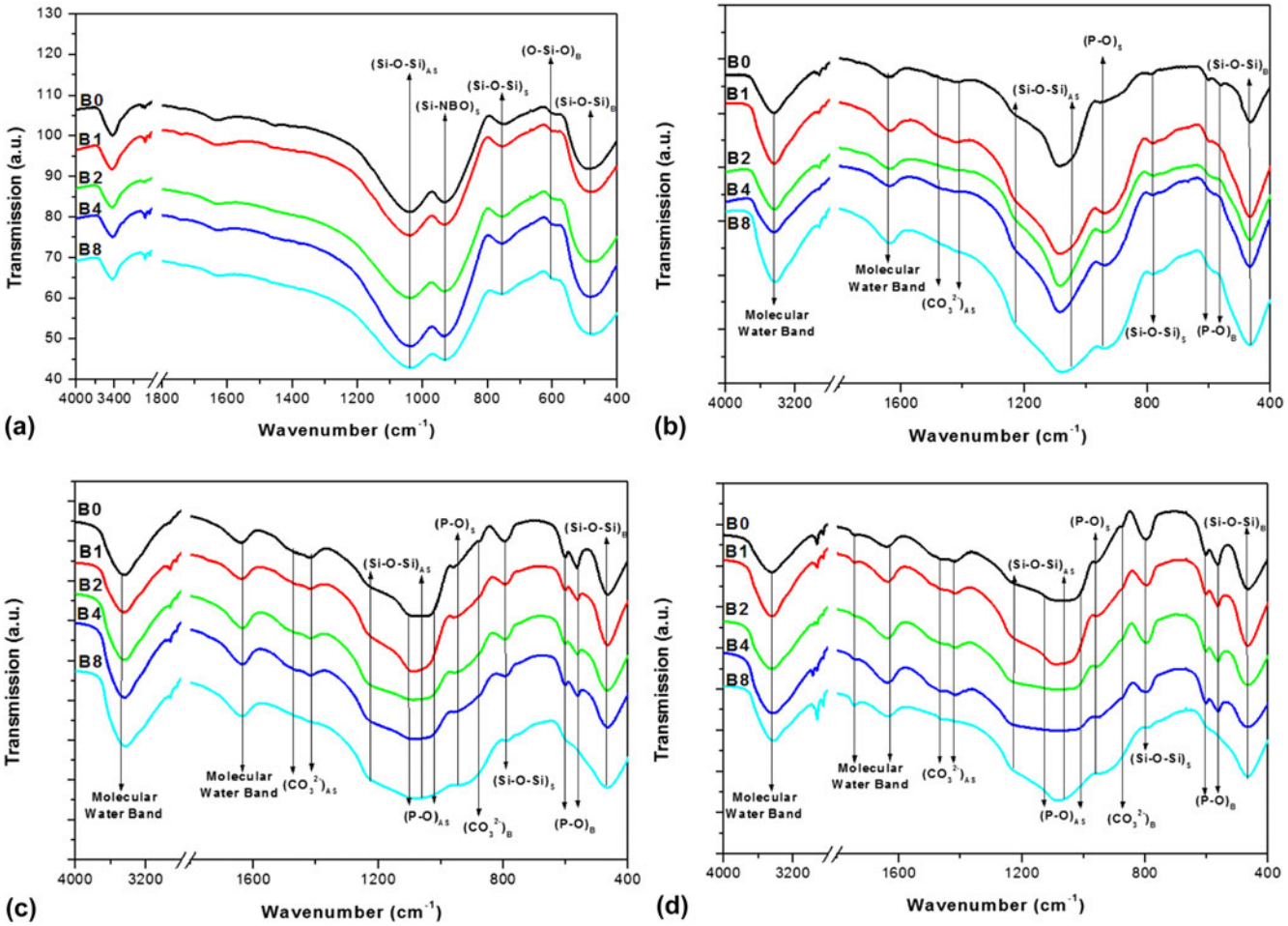


FIG. 2. FTIR transmission spectra of (a) melt-quenched bulk glass samples, glass powders after immersion in the SBF solution for (b) 3 days, (c) 7 days, and (d) 14 days.

it is observed that the vibrational bands are quite similar to those of the glass powders which were immersed in the SBF solution for 7 days.

C. Thermal properties

The DSC thermograms for all the glasses recorded at 10 K/min of rate of heating are shown in Fig. 3. It can be observed that all samples show a distinct endothermic signal corresponding to the glass transition temperature (T_g) followed by a broad exothermic peak corresponding to crystallisation. The glass transition temperature (T_g), crystallisation onset temperature (T_x), and glass stability factor ($\Delta T = T_x - T_g$) for all the glasses are summarised in Table II.

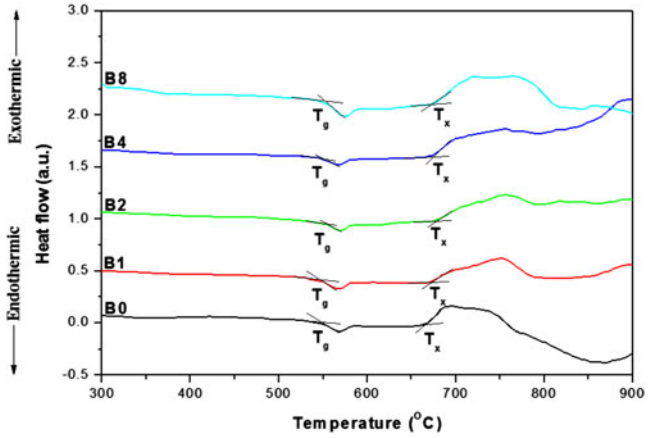


FIG. 3. DSC thermogram of the glass powders recorded at a heating rate of 10 K/min.

D. Density

The measured density values of the glasses are 2.68, 2.69, 2.71, 2.77, and 2.85 g/cc for B0, B1, B2, B4, and B8 samples, respectively. Thus, the variation in the density values indicates that it increases with the gradual substitution of Bi_2O_3. As the density of Bi_2O_3 (8.90 g/cc) is much higher than that of SiO_2 (2.196 g/cc) and Na_2O (2.127 g/cc), the density of glasses increases with the increase in substitution of Bi_2O_3 replacing SiO_2 and Na_2O.

https://doi.org/10.1557/jmr.2017.442 Published online by Cambridge University Press

E. Microstructural studies

FESEM micrographs of all five glass samples immersed in the SBF solution for 7 days are shown in Figs. 4(a)–4(e) which corresponds to B0, B1, B2, B4, and B8 glass samples, respectively. The B0 glass surface shows a flake-like fine microstructure with high porosity, while the average thickness of the flakes is around 60 nm. The surfaces of B1 and B2 glasses show slightly modified rod-like and spherical morphology, respectively. The average diameter of the rod-like structure in the B1 glass surface is around 70 nm, while the average diameter of the spherical particles on the surface of the B2 glass is around 120 nm. However, from FESEM micrographs, it is apparent that porosity decreases in the case of B1 and B2 samples compared to the B0 glass. Even though there is a difference in the surface morphology of B0, B1, B2 glasses, the formation of HAp and HCA was confirmed on the surface of B1 and B2 samples similar to that of the B0 glass as previously observed in Sec. III.A (XRD analysis). The change in morphology of the surface apatite layer may be attributed to the gradual substitution of Bi_2O_3 in the glass. The B8 glass surface after immersion in the SBF solution for 7 days does not seem to contain a precipitated layer of HAp or HCA and may be only having some polymerised silica gel layers on its surface. Section III.A (XRD analysis) also showed similar evidences of formation of the Si–O–Si gel layer.

FESEM images of three selected glasses (B0, B2, and B8) immersed in the SBF solution for 14 days are shown in Figs. 4(f)–4(h), respectively. The surface of the B0 glass sample shows similar morphology to that of immersion in the SBF solution for 7 days, while the morphology changes from spherical to flake-like crystals in case of the B2 glass sample surface.

TABLE II. The values of glass transition temperature (T_g), crystallisation onset temperature (T_x) and glass stability factor (ΔT) for different glasses obtained from their respective DSC thermogram at heating rate of 10 K/min.

Glass	T_g (°C) ± 1	T_x (°C) ± 1	$\Delta T = T_g - T_x$
B0	542	661	119
B1	542	672	130
B2	550	677	127
B4	547	672	125
B8	552	674	122

F. pH and ion release studies

The concentration of Si^{4+}, Na^{+}, and P^{5+} ions released from glasses during immersion in SBF solution has been analyzed from the supernatant collected after 7 and 14 days, and the data is given in Table III. From Table III, it can be observed that the concentration of Si^{4+} ions increases in the SBF supernatant as Bi_2O_3

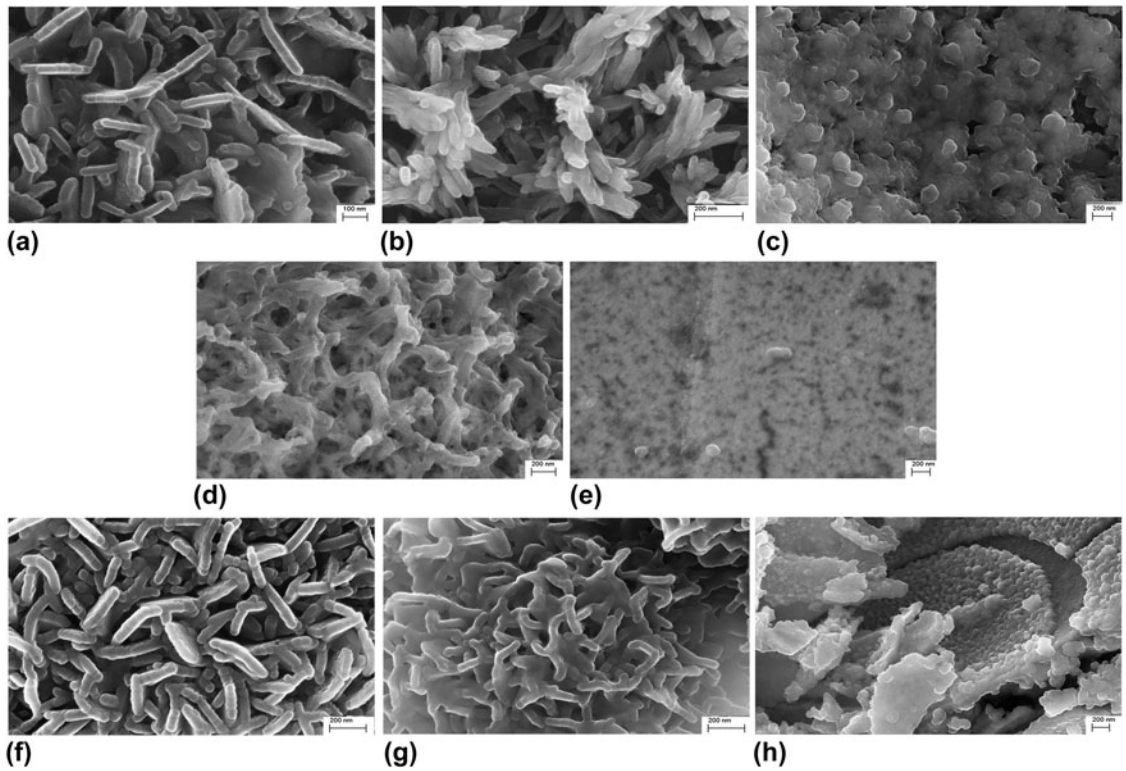


FIG. 4. FESEM micrographs of glass samples immersed in SBF for 7 days, (a) B0, (b) B1, (c) B2, (d) B4, and (e) B8 and for 14 days, (f) B0, (g) B2, and (h) B8.

https://doi.org/10.1557/jmr.2017.442 Published online by Cambridge University Press

TABLE III. Concentration of Si^{4+}, Na^{+}, P^{5+}, and Bi^{3+} ions and pH of SBF supernatant for different immersion time of all glasses.

	Si^{4+} (mg/L)			Na^{+} (mg/L)			P^{5+} (mg/L)			pH ± 0.01		
	Days			Days			Days			Days		
Glass samples	0	7	14	0	7	14	0	7	14	0	7	14
B0	...	37.38	62.58	3309.3	3303.5	3039.5	30.04	5.3	3.96	7.4	7.98	8.05
B1	...	51.24	64.89	3309.3	3252.5	2538.5	30.04	24.81	16.78	7.4	7.88	7.97
B2	...	54.18	67.2	3309.3	3166	2977.5	30.04	23.5	5.19	7.4	7.88	7.95
B4	...	80.85	70.14	3309.3	2857	3266.5	30.04	10	3.58	7.4	7.74	7.79
B8	...	65.52	72.03	3309.3	2911	3085.5	30.04	30.6	33.68	7.4	7.74	7.75

substitution is gradually increased in glass. Generally, Si^{4+} ions are released in small concentrations from the glasses along with the formation of the Si–O–Si gel layer on the glass surface. Also, some Si^{4+} ions in the form of $(SiO_4)^{4-}$ may replace few $(PO_4)^{3-}$ ions in the apatite lattice.[32] Thus, it is expected that with an increase in apatite formation on the surface, there will be an increase in the Si^{4+} ion substitution in apatites. As reported in Sec. III.A (XRD analysis), it was observed that with gradual increase in Bi_2O_3 substitution in the glass composition, apatite formation was gradually reduced. Thus, when the rate of Si^{4+} ion release from glass becomes higher than the rate of Si^{4+} ion substitution in apatites, there might be an increase in Si^{4+} ion concentration in the SBF supernatant. After immersion in the SBF solution for 14 days for the B4 glass, Si^{4+} ion concentration decreases in comparison to the Si^{4+} concentration after 7 days among all glasses studied due to slower surface apatite formation and Si^{4+} substitution in apatites. The highest concentration of Si^{4+} ion is evidenced in the B8 sample after 14 days which is also attributed to the lack of apatite formation.

From Table III, it can be observed that for B0, B1, and B2 glasses, the Na^{+} ions in the supernatant after 14 days is lower compared to the concentration of Na^{+} ions after 7 days. It can be concluded that Na^{+} ions may participate into an apatite structure forming substituted apatites.[32] However, due to the poor apatite forming ability of B4 and B8 glasses, an increase in the concentration of Na^{+} ions in the supernatant is observed after 14 days in comparison to the supernatant after 7 days.

The concentration of P^{5+} ions in the SBF supernatant of all glasses has decreased in comparison to the prepared SBF due to the utilization of these ions for the formation of HAp and HCA layers except the B8 sample. Least apatite formation has been evidenced for the B8 glass resulting in a higher P^{5+} ion concentration in the supernatants.

Figure 5 shows the concentration of Bi^{3+} ions in the supernatant collected after immersing the glass samples in the SBF solution for 7 and 14 days. Interestingly, Bi^{3+} ion release is very low (in ppb range) for all the samples in comparison to other ions due to the comparatively

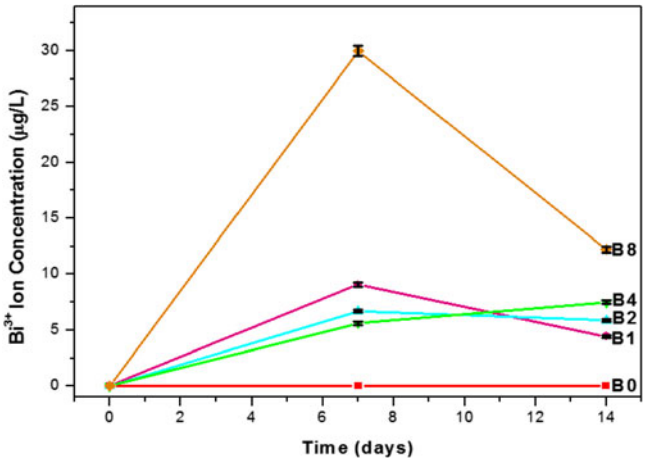


FIG. 5. Concentration of Bi^{3+} ions in the supernatent with different immersion time of all glasses studied in SBF solution.

lower concentration of Bi_2O_3 in the glass composition. After immersion in the SBF solution for 7 days, the highest release of Bi^{3+} ions is observed in case of the B8 sample. For other Bi_2O_3-substituted glasses, their SBF supernatant shows a lower Bi^{3+} ion concentration than that of the B8 glass sample. However, after immersion for 14 days, the Bi^{3+} ion concentration increases in the supernatant with the gradual increase of Bi_2O_3 in the glass composition. Glasses B1 and B2 show higher Bi^{3+} ion concentration in the supernatant after 7 days compared to that of 14 days. This may occur due to the participation of some released Bi^{3+} ions into the apatite lattice during immersion for 7 days.[20,21]

The pH values measured from the SBF supernatant collected after 7 and 14 days are reported in Table III. Compared to the pH values of SBF supernatants after 7 days, there is an increase in the pH values with that of 14 days. It can also be observed that the pH values gradually decrease with the increase in Bi_2O_3 substitution in glasses after both 7 and 14 days.

G. Cell proliferation studies

The cell proliferation (%) of NIH3T3 mouse fibroblast cells on the surface of B0, B1, B2, B4, and B8 glass samples for 3, 7, and 11 days has been estimated from the

https://doi.org/10.1557/jmr.2017.442 Published online by Cambridge University Press

OD values obtained through an MTT assay, and the plotted data is shown in Fig. 6. The base glass (B0) was considered as the control. All calculated P values showed statistically highly significant results ($P < 0.001$) compared to the base glass (B0). It can be observed that among Bi_2O_3-substituted glasses, cell proliferation is higher for 1 wt% Bi_2O_3 substitution and decreases with further increase in Bi_2O_3 substitution in all the time periods studied. After 3 days, the B1 glass shows a marginally higher cell proliferation (%) than that of cells on the base glass (B0), whereas cell proliferation is less in B2 and B4 glasses compared to the base glass. The least cell proliferation (%) was evidenced on the B8 sample indicating the adverse effect of Bi^{3+} ions on cell proliferation. After 7 days, cell proliferation rates on all the Bi_2O_3-substituted glasses are lower than those of the base glass (B0). But after 11 days, the cell proliferation (%) is higher for B1 and B2 glasses and gradually decreases in B4 and B8 glasses. However, there is an increase in cell proliferation after 11 days compared to 7 days for all the Bi_2O_3-substituted glasses.

H. Antibacterial studies

The change in optical density (ΔOD) values obtained for all the glass powders-added *E. coli* bacterial suspensions from the broth microdilution method was used to understand the bacteriostatic effects of the glass samples. Figure 7 shows the comparison of ΔOD values of glass powders-added *Escherichia coli* (*E. coli*) bacterial suspensions after 1 and 2 h of incubation with ΔOD values of the base glass (B0) as the positive control and ΔOD of the only *E. coli* bacterial suspension as the negative control. From the Student's t-test analysis, it is ensured that all the samples exhibited statistically significant results ($P < 0.05$) compared to the negative control. It can be observed that all the Bi_2O_3-substituted glasses as well as the base glass (B0) has shown a bacteriostatic effect on the *E. coli* bacteria after 1 and 2 h of incubation when compared with the negative control.

The bactericidal properties of the glass powders were studied by counting the CFU on cultured agar plates spread with the glass powders-added bacterial suspension. Figure 8 shows the cultured agar plates spread with different glass powders-added bacterial suspensions incubated for 24 h. Each image in Fig. 8 contains one cultured agar plate for positive control (+) and another cultured agar plate for negative control (−) along with the cultured agar plates for Bi_2O_3-substituted glasses in triplicates. On observing the CFU present on the respective agar plates of Bi_2O_3-substituted glasses, it can be concluded that B1 glass powders having 1 wt% Bi_2O_3 substitution have caused bactericidal activity on the *E. coli* bacteria. There are no CFUs present in the cultured agar plates applied with 24 h incubated B1 glass powders-added bacterial suspension while "too numerous to count" (TNTC) CFUs are present on agar plates applied with glass samples having Bi_2O_3 substitution above 1 wt%. The positive-control and negative-control agar plates in the entire images show TNTC colony-forming units (CFU) as observed in Fig. 8.

IV. DISCUSSION

The XRD and FTIR results of as-prepared glasses have shown the amorphous nature of the glasses and absence

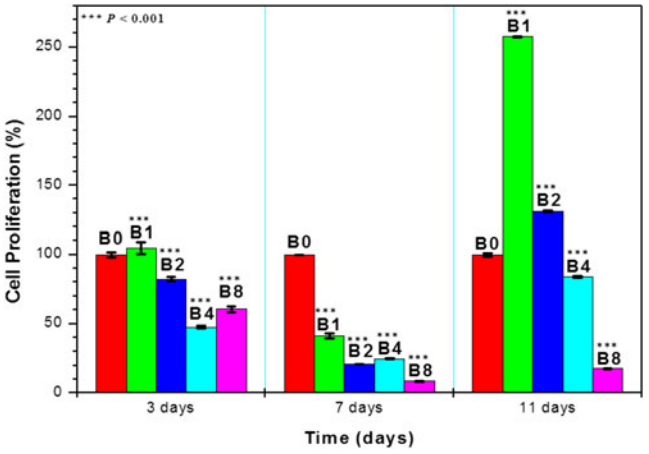


FIG. 6. Cell proliferation (%) of NIH3T3 mouse fibroblast cells on the surface of different glass samples plotted using MTT assay results and taking the base glass (B0) as control. Data are expressed as mean cell proliferation (%) ± SE. Statistical significance was determined by using the P value from Student's t-test (one-tailed hypothesis with two independent samples having equal variance). Samples show statistical differences for all the samples relative to the base glass (B0) as control at ***$P < 0.001$.

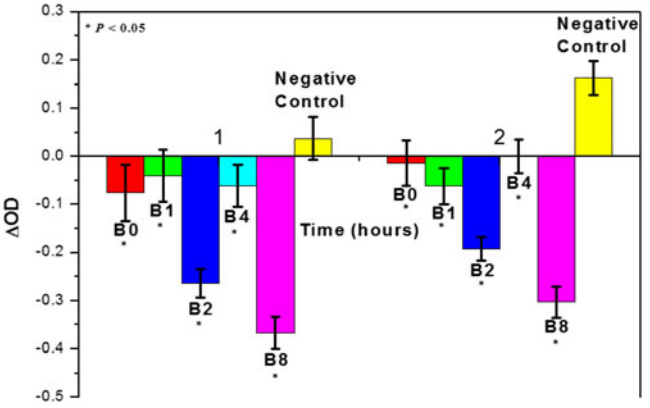


FIG. 7. Plot of ΔOD values of the different glass powders added bacterial suspension after incubation for 1 and 2 h with base glass (B0) as positive control and only bacterial suspension as negative control. Data are expressed as mean ΔOD values ±SE. Statistical significance was determined by using the P value from Student's t-test (one-tailed hypothesis with two independent samples having equal variance). Samples show statistical differences for all the samples relative to the negative control at *$P < 0.05$.

https://doi.org/10.1557/jmr.2017.442 Published online by Cambridge University Press

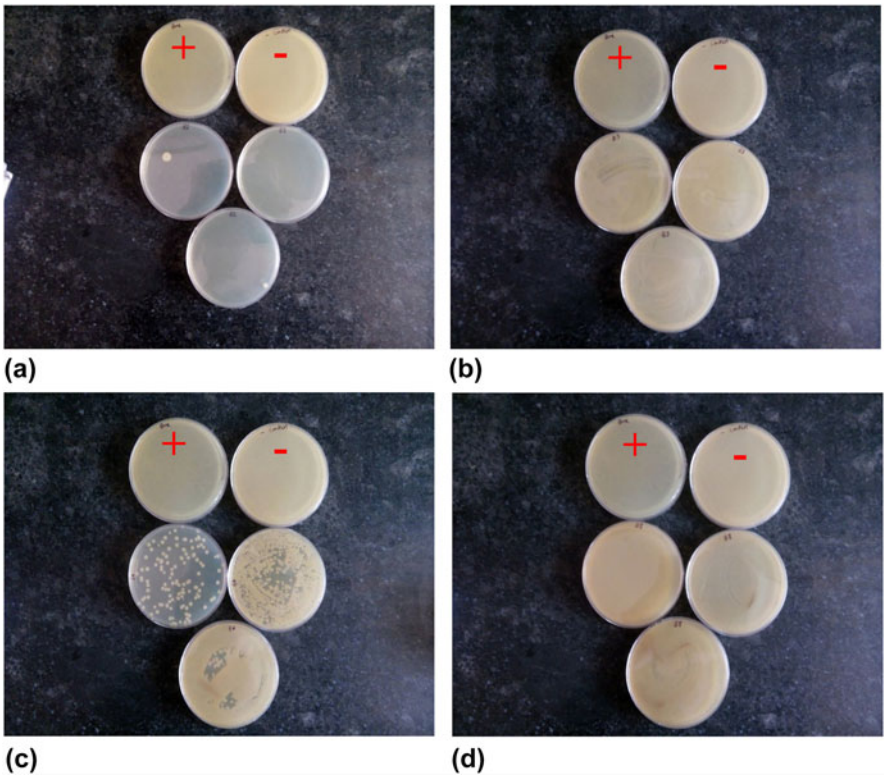


FIG. 8. Overnight cultured agar plates: (+) denotes positive control, (−) denotes negative control and three agar plates applied with 24 h incubated glass powders [(a) B1, (b) B2, (c) B4, and (d) B8] added *E. coli* bacterial suspension.

of significant structural changes in the glasses, respectively. However, it should be noted that in FTIR spectra of bismuth oxide containing glasses, the stretching vibrations related to Bi–O bond in distorted BiO_6 units (490–500 cm^{-1}) could be overlapped with Si–O–Si and O–Si–O bending vibrational bands. Also, the symmetric stretching vibrations of Bi–O bond in BiO_3 units at 840–880 cm^{-1} may also be overlapped with the broad and intense vibrational bands associated with Si-NBO stretching.[33,34] After SBF immersion studies, XRD, FTIR and FESEM studies showed similar results where substitution of Bi_2O_3 upto 2 wt% had no adverse effect on surface apatite forming ability of modified glasses but significant reduction in surface apatite formation could be seen for the glasses with Bi_2O_3 substitution higher than 4 wt%. With the gradual increase in Bi_2O_3 concentration in glass, the poor apatite forming ability is attributed to the increased network connectivity on account of the reduction in non-bridging oxygen associated with the decrease in Na_2O content in the glasses. The results obtained during present bioactivity studies contradict with the results obtained by Mohn et al. who reported improved apatite formation for Bi_2O_3 added nano-bioactive glass powders.[23] However, in their studies, the actual role of Bi^{3+} ions in the glass network was not reported.

To understand the glass stability, the crystalline phase formed during heating was investigated for which selected glass samples were heat treated at 725 °C, and the corresponding phase was identified as $Na_2Ca_2Si_3O_9$ (JCPDS 22-1455) from their XRD patterns (not shown). Similar phase formation upon heat treatment was reported by Fujikura et al. and Massera et al.[35,36] The glass stability factor plays a significant role in scaffold processing or sintering as the glassy phase should not get devitrified when heated above T_g.[37] The well-known 45S5 glass exhibits a ΔT value of 88 °C and is prone to crystallisation forming the $Na_2CaSi_2O_6$ crystalline phase while scaffold processing.[35] Bismuth oxide-modified glasses have higher ΔT values than that of base glass (B0) as well as 45S5 glass, indicating their suitability in scaffold processing without devitrification.

The concentration of Bi^{3+} ions released from the Bi_2O_3-substituted glasses is in the ppb range, which could be due to lower concentration of Bi_2O_3 in glasses and participation of the Bi^{3+} ion as the network former through $[BiO_3]$ and $[BiO_6]$ polyhedral structural units instead of the network modifier.

The fibroblast cells were used in the present cell proliferation studies due to their wide acceptability in cell viability and toxicity studies for several decades.[38] The results obtained in ion release studies and pH measurements could be correlated to understand the cell compatibility and antibacterial properties of the glasses. The pH values decrease with a gradual increase in Bi_2O_3

https://doi.org/10.1557/jmr.2017.442 Published online by Cambridge University Press

substitution in glass, and improved cell proliferation has been observed at a slightly increased pH.[39,40] However, after 3 days of cell growth, the B1 glass showed a slightly higher cell proliferation compared to the base glass (B0). This could be due to the formation of Bi-substituted HAp, as it has been reported that the incorporation of Bi^{3+} ions substituting the Ca^{2+} ions in the apatite improves the cell viability.[20] Though, Bi-substituted HAp formation was similar in B1 and B2 glasses, the B1 glass showed better cell proliferation than the B2 glass due to a slightly higher pH value. Also, there is a possibility that the high concentration of Bi^{3+} ions can also affect the cell proliferation. For B4 and B8 glasses, lower pH changes with that of the growth media (7.4), reduced the surface apatite-forming ability, and higher Bi^{3+} ion concentration could have resulted in lower cell proliferation compared to B0, B1, and B2 glasses. After 7 days, there is a decrease in cell proliferation on all the Bi_2O_3-substituted glasses though the surface apatite and pH values are expected to increase compared to that of 3 days. This could be only due to the increase in Bi^{3+} ion concentration in the surrounding medium. After cell proliferation studies for 11 days, the higher cell proliferation in B1 and B2 glasses compared to the base glass (B0) is related to the decrease in the Bi^{3+} ion concentration in the SBF supernatant between 7 and 14 days as revealed in the ion concentration studies. It should be noted that bismuth compounds on excessive intake are associated with neurological toxicity like encephalopathy and nephrological problems like renal failures.[41,42] However, it has been reported that the blood level of the Bi^{3+} ion in humans below 50 ppb was unlikely to induce toxicity.[42] The Bi^{3+} ion concentrations measured from SBF supernatants after 7 and 14 days are lower (4.4–9.1 ppb) for all the bismuth-oxide substituted glasses except B8 (12.24–30 ppb), corroborating the lowest cell compatibility of the B8 sample.

To evaluate the antibacterial action of the developed glasses, a Gram-negative *Escherichia coli* (*E. coli*) was selected instead of the Gram-positive bacterium for the preliminary study to understand the efficacy of bismuth ions. As the Gram-positive bacterium (e.g., *S. aureus*) possesses a thicker cell wall and more peptidoglycan molecules; the action of the antibacterial ions is more susceptible in the Gram-negative bacterium compared to the Gram-positive bacterium.[43] The bacterial growth inhibition is expected to occur due to the increase in the pH value of the surrounding medium for bioactive glasses.[8] Also, Bi_2O_3-substituted glasses release Bi^{3+} ions into the surrounding medium which can bring in possible inhibition to the bacterial cells. The base glass (B0) showed higher inhibition than the B1 glass after 1 h, which is attributed to the increased pH change as shown in Table III. However, it is important to mention that in case of the B2 sample, though the change in pH value was decreased, a stronger inhibition is observed compared to B0 and B1 glasses due to the probable antibacterial action of Bi^{3+} ions rather than the pH effect. In case of the B8 glass, though it exhibits the least pH change compared to the pH of MHB, the higher Bi^{3+} ion release influenced the bacterial inhibition. Moreover, except the B1 glass, all the other glass samples exhibited a decrease in the ΔOD value of 2 h compared to 1 h. This could be due to the simultaneous influence of pH changes as well as the antibacterial action of Bi^{3+} ions, creating the strongest inhibitory effect toward the bacteria in the B1 glass. Interestingly, the B1 sample also demonstrated bactericidal properties as revealed in agar plate studies. Further, this can be evidenced from the fact that only the B1 glass showed continuous increase in bacterial inhibition while for other glasses, the bacterial inhibition was decreased with time.

As the B1 glass showed encouraging bacteriostatic and bactericidal effects on Gram-negative *E. coli*, the evaluation of bacteriostatic and bactericidal action of this glass is intended to be evaluated against the Gram-positive bacteria (e.g., *S. aureus*) in future, which may also give an insight about the possible antibacterial action of penetration through the cell wall.

V. CONCLUSIONS

In the present work, Bi_2O_3 modified glasses substituting SiO_2 and Na_2O equally with 1, 2, 4, and 8 wt% Bi_2O_3 have been synthesized using the conventional melt-quenching technique. XRD analysis of the as-cast glasses confirmed the amorphous nature of the glasses, while FTIR spectroscopy does not reveal any noticeable changes among the glasses due to the possible overlapping of the bands related to the stretching of BiO_3 and BiO_6 units with that of Si–O–Si stretching and bending bands. From DSC analysis, it could be observed that the glass transition temperature does not show major changes, while the glass stability factor (ΔT) for all the Bi_2O_3-containing glasses is higher than that of the base glass. Density of the glasses increases with a gradual increase in Bi_2O_3 substitution due to the higher density of Bi_2O_3 compared to SiO_2 or Na_2O. After SBF immersion for 7 and 14 days, it is observed that the surface apatite forming ability decreases with the gradual substitution of Bi_2O_3 in glasses as evidenced from XRD, FTIR, and FESEM studies. The B8 glass having the highest Bi_2O_3 content did not show any apatite formation up to 14 days of SBF immersion, which is attributed to the increased network connectivity. The release of Bi^{3+} ions into SBF for all the glasses is limited in the ppb level (4–30 μg/L). All the Bi_2O_3 modified glasses exhibit a bacteriostatic effect on the *E. coli* bacteria after 1 and 2 h of incubation. In particular, the 1 wt% Bi_2O_3-containing glass shows better cell proliferation rates as well as bactericidal

https://doi.org/10.1557/jmr.2017.442 Published online by Cambridge University Press

properties compared to the base glass. This study infers that the inclusion of bismuth ions (1 wt%) into commercial glasses like (S53P4) could be beneficial with a desired combination of optimized apatite formation on the surface, cell compatibility and antibacterial properties. Finally, it can be concluded that Bi_2O_3 being a widely used radiopacifier can be a potential additive to bioactive glasses along with its antibacterial properties.

ACKNOWLEDGMENTS

Authors would like to express their grateful thanks to Dr. K. Muraleedharan, Director, CSIR-CGCRI and Dr. Ranjan Sen, Head, Glass division for their encouragement and support toward this work. The financial help from P 81-113 of the CSIR Extramural Research Fund for Young Scientists and CSIR-HRDG (Extramural Research Group) for providing GATE-JRF fellowship to SPS for pursuing Integrated M.Tech Ph.D. program is gratefully acknowledged. The authors gratefully acknowledge the suggestions and experimental help offered by Dr. Biswanath Kundu, Senior Scientist and Dr. Vamsi K. Balla, Senior Principal Scientist, Bioceramics and Coating Division, CSIR-CGCRI.

REFERENCES

1. L.L. Hench and J.R. Jones: Bioactive glasses: Frontiers and challenges. *Front. Bioeng. Biotechnol.* **3**, 1 (2015).
2. L.L. Hench: The story of Bioglass®. *J. Mater. Sci.: Mater. Med.* **17**, 967 (2006).
3. Ö.H. Andersson, G. Liu, K.H. Karlsson, L. Niemi, J. Miettinen, and J. Juhanoja: In vivo behaviour of glasses in the SiO_2–Na_2O–CaO–P_2O_5–Al_2O_3–B_2O_3 system. *J. Mater. Sci.: Mater. Med.* **1**, 219 (1990).
4. M. Brink, T. Turunen, R-P. Happonen, and A. Yli-Urpo: Compositional dependence of bioactivity of glasses in the system Na_2O–K_2O–MgO–CaO–B_2O_3–P_2O_5–SiO_2. *J. Biomed. Mater. Res., Part A* **37**, 114 (1997).
5. D.P. Lew and F.A. Waldvogel: Osteomyelitis. *Lancet* **364**, 369 (2004).
6. G. Sakoulas and R.C. Moellering: Increasing antibiotic resistance among methicillin-resistant *Staphylococcus aureus* strains. *Clin. Infect. Dis.* **46**, S360 (2008).
7. W-T. Jia, Q. Fu, W-H. Huang, C-Q. Zhang, and M.N. Rahaman: Comparison of borate bioactive glass and calcium sulfate as implants for the local delivery of teicoplanin in the treatment of methicillin-resistant *Staphylococcus aureus*-induced osteomyelitis in a rabbit model. *Antimicrob. Agents Chemother.* **59**, 7571 (2015).
8. I. Allan, H. Newman, and M. Wilson: Antibacterial activity of particulate Bioglass® against supra-and subgingival bacteria. *Biomaterials* **22**, 1683 (2001).
9. M. Bellantone, H.D. Williams, and L.L. Hench: Broad-spectrum bactericidal activity of Ag_2O-doped bioactive glass. *Antimicrob. Agents Chemother.* **46**, 1940 (2002).
10. H. Zhu, C. Hu, F. Zhang, X. Feng, J. Li, T. Liu, J. Chen, and J. Zhang: Preparation and antibacterial property of silver-containing mesoporous 58S bioactive glass. *Mater. Sci. Eng., C* **42**, 22 (2014).
11. M. Ottomeyer, A. Mohammadkah, D. Day, and D. Westenberg: Broad-spectrum antibacterial characteristics of four novel borate-based bioactive glasses. *Adv. Microbiol.* **6**, 776 (2016).
12. A.M. Mulligan, M. Wilson, and J.C. Knowles: Effect of increasing silver content in phosphate-based glasses on biofilms of *Streptococcus sanguis*. *J. Biomed. Mater. Res., Part A* **67**, 401 (2003).
13. E.A.A. Neel, I. Ahmed, J. Pratten, S.N. Nazhat, and J.C. Knowles: Characterisation of antibacterial copper releasing degradable phosphate glass fibres. *Biomaterials* **26**, 2247 (2005).
14. A.M. Mulligan, M. Wilson, and J.C. Knowles: The effect of increasing copper content in phosphate-based glasses on biofilms of *Streptococcus sanguis*. *Biomaterials* **24**, 1797 (2003).
15. Y-F. Goh, A.Z. Alshemary, M. Akram, M.R.A. Kadir, and R. Hussain: In vitro characterization of antibacterial bioactive glass containing ceria. *Ceram. Int.* **40**, 729 (2014).
16. D.W. Bierer: Bismuth subsalicylate: History, chemistry, and safety. *Rev. Infect. Dis.* **12**, S3 (1990).
17. J.R. Lambert and P. Midolo: The actions of bismuth in the treatment of *Helicobacter pylori* infection. *Aliment. Pharmacol. Ther.* **11**, 27 (1997).
18. M. Parirokh and M. Torabinejad: Mineral trioxide aggregate: A comprehensive literature review—Part I: Chemical, physical, and antibacterial properties. *J. Endod.* **36**, 16 (2010).
19. M. Torabinejad and M. Parirokh: Mineral trioxide aggregate: A comprehensive literature review—Part II: Leakage and biocompatibility investigations. *J. Endod.* **36**, 190 (2010).
20. T.J. Webster, E.A. Massa-Schlueter, J.L. Smith, and E.B. Slamovich: Osteoblast response to hydroxyapatite doped with divalent and trivalent cations. *Biomaterials* **25**, 2111 (2004).
21. G. Ciobanu, A.M. Bargan, and C. Luca: New bismuth-substituted hydroxyapatite nanoparticles for bone tissue engineering. *JOM* **67**, 2534 (2015).
22. S. Heid, P.R. Stoessel, T.T. Tauböck, W.J. Stark, M. Zehnder, and D. Mohn: Incorporation of particulate bioactive glasses into a dental root canal sealer. *Biomed. Glasses* **2**, 29 (2016).
23. D. Mohn, M. Zehnder, T. Imfeld, and W.J. Stark: Radio-opaque nanosized bioactive glass for potential root canal application: Evaluation of radiopacity, bioactivity and alkaline capacity. *Int. Endontic. J.* **43**, 210 (2010).
24. T. Kokubo, H. Kushitani, S. Sakka, T. Kitsugi, and T. Yamamuro: Solutions able to reproduce in vivo surface-structure changes in bioactive glass-ceramic A–W^3. *J. Biomed. Mater. Res.* **24**, 721 (1990).
25. S.A. Bernard, V.K. Balla, N.M. Davies, S. Bose, and A. Bandyopadhyay: Bone cell–materials interactions and Ni ion release of anodized equiatomic NiTi alloy. *Acta Biomater.* **7**, 1902 (2011).
26. S. Bodhak, V.K. Balla, S. Bose, A. Bandyopadhyay, U. Kashalikar, S.K. Jha, and S. Sastri: In vitro biological and tribological properties of transparent magnesium aluminate (Spinel) and aluminum oxynitride (ALON®). *J. Mater. Sci.: Mater. Med.* **22**, 1511 (2011).
27. J.M. Andrews: Determination of minimum inhibitory concentrations. *J. Antimicrob. Chemother.* **48**, 5 (2001).
28. X. Ou, S. Xu, J.M. Warnett, S.M. Holmes, A. Zaheer, A.A. Garforth, M.A. Williams, Y. Jiao, and X. Fan: Creating hierarchies promptly: Microwave-accelerated synthesis of ZSM-5 zeolites on macrocellular silicon carbide (SiC) foams. *Chem. Eng. J.* **312**, 1 (2017).
29. K.M. El Badry, F.A. Moustaffa, M.A. Azooz, and F.H. El Batal: Infrared absorption spectroscopy of some bio-glasses before and after immersion in various solutions. *Indian J. Pure Appl. Phys.* **38**, 741 (2000).
30. S. Koutsopoulos: Synthesis and characterization of hydroxyapatite crystals: A review study on the analytical methods. *J. Biomed. Mater. Res.* **62**, 600 (2002).
31. F.Z. Ren and Y. Leng: Carbonated apatite, type-A or type-B? *Key Eng. Mater.* **493**, 293 (2012).

https://doi.org/10.1557/jmr.2017.442 Published online by Cambridge University Press

32. D.M. Ibrahim, A.A. Mostafa, and S.I. Korowash: Chemical characterization of some substituted hydroxyapatites. *Chem. Cent. J.* **5**, 74 (2011).
33. I. Ardelean, S. Cora, and V. Ioncu: Structural investigation of $CuO–Bi_2O_3–B_2O_3$ glasses by FT-IR, Raman and UV-VIS spectroscopies. *J. Optoelectron. Adv. Mater.* **8**, 1843 (2006).
34. F. He, Z. He, J. Xie, and Y. Li: IR and Raman spectra properties of $Bi_2O_3–ZnO–B_2O_3–BaO$ quaternary glass system. *Am. J. Anal. Chem.* **5**, 1142 (2014).
35. J. Massera, S. Fagerlund, L. Hupa, and M. Hupa: Crystallization mechanism of the bioactive glasses, 45S5 and S53P4. *J. Am. Ceram. Soc.* **95**, 607 (2012).
36. K. Fujikura, N. Karpukhina, T. Kasuga, D.S. Brauer, R.G. Hill, and R.V. Law: Influence of strontium substitution on structure and crystallisation of Bioglass® 45S5. *J. Mater. Chem.* **22**, 7395 (2012).
37. X. Wang, S. Fagerlund, J. Massera, B. Södergård, and L. Hupa: Do properties of bioactive glasses exhibit mixed alkali behavior? *J. Mater. Sci.* **52**, 8986 (2017).
38. K.C. da Silva Gasque, L.P. Al-Ahj, R.C. Oliveira, and A.C. Magalhães: Cell density and solvent are critical parameters affecting formazan evaluation in MTT assay. *Braz. Arch. Biol. Technol.* **57**, 381 (2014).
39. C.R. Kruse, M. Singh, S. Targosinski, I. Sinha, J.A. Sørensen, E. Eriksson, and K. Nuutila: The effect of pH on cell viability, cell migration, cell proliferation, wound closure, and wound reepithelialization: In vitro and in vivo study. *Wound Repair Regen.* **25**, 260 (2017).
40. A-M. Galow, A. Rebl, D. Koczan, S.M. Bonk, W. Baumann, and J. Gimsa: Increased osteoblast viability at alkaline pH in vitro provides a new perspective on bone regeneration. *Biochem. Biophys. Rep.* **10**, 17 (2017).
41. F. Thomas, B. Bialek, and R. Hensel: Medical use of bismuth: The two sides of the coin. *J. Clin. Toxicol.* **S3**, 495 (2011).
42. P.T. Reynolds, K.C. Abalos, J. Hopp, and M.E. Williams: Bismuth toxicity: A rare cause of neurologic dysfunction. *Int. J. Clin. Med.* **3**, 46 (2012).
43. Q.L. Feng, J. Wu, G.Q. Chen, F.Z. Cui, T.N. Kim, J.O. Kim, T.N. Kim, and J.O. Kim: A mechanistic study of the antibacterial effect of silver ions on *Escherichia coli* and *Staphylococcus aureus*. *J. Biomed. Mater. Res.* **52**, 662 (2000).

https://doi.org/10.1557/jmr.2017.442 Published online by Cambridge University Press